On the Description of Hardening and Softening Effects in the Austenitic Steel Type 304 (WN 1.4948)

G.T.M. Janssen

TNO, Institute for Mechanical Constructions, P.O. Box 29, NL-2600 AA Delft, The Netherlands

Summary

Constitutive equations were developed to describe plastic deformations in the framework of the TNO-research programme on inelastic analysis of structural components within the SNR-300 fast breeder reactor. Two types of steel, the austenitic steel WN 1.4948 and the ferritic steel WN 1.6770 were investigated. The experimental verification of the mathematical description was performed for biaxial states of stress but also for cyclic and non-radial load histories. The description of plastic deformation was based on the so-called fraction model of BESSELING, in some cases indicated as sub-layer or overlay model.

It was concluded that the main source of the discrepancies between the theory and experiments on the austenitic steel (WN 1.4948) could be found in the description of the gradual transition from elastic to fully plastic behaviour after a load reversal. During this transition process the isotropic hardening plays an important role in the steel considered. It was also found that during cyclic straining the linear elastic range diminishes when the number of cycles increases. This effect can be considered as a softening effect. So, it may be stated that in the transition region we have to do with competing processes of hardening and softening. Consequently, the curvature in the transition region after a load reversal is much smaller than one would expect observing the curvature of the transition region in the initial load curve.

This paper discusses the mathematical description of these effects, including the determination of the model parameters.

1. Introduction

Constitutive equations were developed to describe plastic deformations in the framework of the TNO-research programme on inelastic analysis of structural components within the SNR-300 fast breeder reactor. Two types of steels, the austenitic steel WN 1.4948 and the ferritic steel WN 1.6770 were investigated [2, 3, 4, 5]. The experimental verification of the mathematical description was performed for biaxial states of stress but also for cyclic and non-radial load histories. The description of the plastic deformation including strain hardening and strain rate effects was based on the so-called fraction model of BESSELING [1], in some cases indicated as sub-layer or overlay model. A uni-axial picture of such a model for time-independent plastic deformation is shown in Fig. 1.

It was concluded that the main origin of the discrepancies between theory and experiments on the austenitic steel WN 1.4948 is the gradual transition from elastic to fully plastic behaviour after a load reversal. During this transition process the isotropic hardening plays an important role in the steel considered. It was also found that during cyclic straining the linear elastic range diminishes when the number nf cycles increases. This effect may be considered as a softening effect. So, it may be stated that in the transition region we have to do with competing processes of hardening and softening. Consequently, the curvature in the transition region after a load reversal is much smaller than one would expect on the basis of isotropic and/or kinematic hardening rules.

This paper briefly discusses a mathematical description of these effects. This model can describe, at least qualitatively, the effects as shown in Figs 3, 6 and 8. Fig. 6 shows the LÜDERS-strain in the initial load curve of mild steel, accompanied by the occurrence of an upper and a lower yield stress. After the first load reversal the softening is exhausted and the steel shows a gradual and smooth transition from elastic to plastic behaviour.

Fig. 8 shows the results of a cyclic torsion test on an austenitic steel. The linear elastic stress range after a load reversal becomes smaller when the cycle number increases. It looks like a decrease of YOUNG's modulus after some load cycles.

Fig. 3 shows that the hardening behaviour is influenced by the strain range. For small strain ranges the amount of hardening is very small. When after saturation of isotropic hardening the strain range is increased, the material again shows isotropic hardening. The amount of hardening, however, is larger than before and less load cycles are needed to arrive at the state of exhausted hardening. Fig. 4 shows the stress amplitude of this test (A08A1) as function of the cycle number. In this figure the experimental results of the one-specimen test are compared with results of constant strain range tests on separate specimens (4 specimens). This strain range effect can also be quantitatively described with the fraction model as is shown in Fig. 5.

2. Theoretical description of hardening and softening

An extensive discussion of the description of the BESSELING-model for plastic deformation including hardening and strain rate effects can be found in [3, 4, 5]. For simplicity's sake we now consider only isothermal load histories and we do neither take into account strain rate nor creep effects.

In that case the incremental stress-strain relation reads [5]:

$$\Delta\sigma_{ij} = [E_{ijmn} - \sum_{k=1}^{N} \psi^k (1-h^k) Y^k_{ijmn}] \Delta\varepsilon_{mn} \qquad (1)$$

in which:

σ_{ij} = total stress tensor;

ε_{ij} = total strain tensor which is the same for all volume fractions;

ψ^k = relative size of volume fraction k. The sum of all fractions is unity;

N = number of volume fractions;

E_{ijmn} = tensor of elastic constants, which is the same for all volume fractions;

Y^k_{ijmn} = yield tensor of volume fraction k and exists only when the state of stress remains in the yield surface in stress space σ^k_{ij};

h^k = isotropic hardening parameter of volume fraction k.

Isotropic hardening parameter h^k is normally a small positive scalar and can be expressed as a function of plastic modulus E^{pk}, as:

$$h^k = \frac{E^{pk}}{E^{pk} + B^k} \qquad (2)$$

where B^k is defined in [5] and is 3G when we adopt the VON MISES-yield surface (G is the shear modulus). The plastic modulus is determined by:

$$E^{pk} = \frac{d\bar{\sigma}^{yk}}{d\bar{\varepsilon}^{pk}} \qquad (3)$$

where we assume that yield stress of volume fraction k, $\bar{\sigma}^{yk}$, is only a function of accumulated equivalent plastic strain $\bar{\varepsilon}^{pk}$:

$$\bar{\varepsilon}^{pk} = \int_o^t \left(\frac{2}{3} \dot{\varepsilon}^{pk}_{ij} \dot{\varepsilon}^{pk}_{ij}\right)^{\frac{1}{2}} dt \qquad (4)$$

in which $\dot{\varepsilon}^{pk}_{ij}$ is the plastic strain rate tensor.

As shown in [4, 5] current yield stress $\bar{\sigma}^{yk}$ can be described satisfactorily by the following exponential expression:

$$\bar{\sigma}^{yk} = \bar{\sigma}^{yk}_o + \sum_{i=1}^{M} \Delta\bar{\sigma}^{yk}_i \left\{1 - \exp\left(\frac{-\bar{\varepsilon}^{pk}}{\bar{\varepsilon}^k_i}\right)\right\} \qquad (5)$$

where M is normally one or two. The initial yield stress of volume fraction k, $\bar{\sigma}_o^{yk}$, the increment of isotropic strain hardening towards saturation, $\Delta\bar{\sigma}_i^{yk}$, and the strain constant, $\bar{\varepsilon}_i^k$, which equals the accumulated strain where 63 percent of the isotropic hardening $\Delta\bar{\sigma}_i^{yk}$ has been gained, have to be determined experimentally. At fraction level we have only isotropic hardening. Anisotropic hardening is introduced by the interaction of the volume fractions causing a self-balancing system of initial stresses. Softening can simply be obtained by introduction of negative values for $\Delta\bar{\sigma}_i^{yk}$ (Fig. 7).

4. Determination of the model parameters

The results of about thirty biaxial tests on the austenitic steel show that yield surfaces can be described satisfactorily by the VON MISES-criterion [3, 4]:

$$\phi^k = \frac{1}{2} s_{ij} s_{ij} - \frac{1}{3} (\bar{\sigma}^{yk})^2 = 0 \qquad (6)$$

where s_{ij} is the deviatoric stress tensor. Current yield stress $\bar{\sigma}^{yk}$ is considered to be a function of the accumulated plastic strain and is formulated by Eq. (5). The determination of the model parameters for saturating strain hardening and softening is still a subject of investigation. For the time being the parameters are determined in a iterative way. Two starting points are being investigated:

(1) A cyclic constant strain amplitude test with a suitable large strain range (Fig. 8).

(2) A cyclic test of the type as shown in Fig. 3.

In the first procedure the stress amplitude of the cyclic test (Fig. 8) has to be plotted as a function of the accumulated plastic strain (Fig. 9) and has to be approximated by the expression:

$$\sigma^y = \bar{\sigma}_o^y + \Delta\bar{\sigma}_1^y \left\{1 - \exp\left(\frac{-\bar{\varepsilon}^p}{\bar{\varepsilon}_1}\right)\right\} \quad ; \quad M = 1 \qquad (7)$$

The next step is to distribute hardening increment $\Delta\bar{\sigma}_1^y$ over all volume fractions in such a way that the following equation is satisfied:

$$\Delta\bar{\sigma}_1^y = \sum_{k=1}^{N} \phi^k \Delta\bar{\sigma}_1^{yk} \qquad (8)$$

A first guess is to assume the same amount of hardening for each volume fraction:

$$\Delta\bar{\sigma}_1^{yk} = \Delta\bar{\sigma}_1^y \qquad (9)$$

Theoretical results based on this hardening distribution are shown in Fig. 10 and compared with experimental ones. The transition from elastic to plastic behaviour has not been very well predicted. A distribution which improves this aspect is:

$$\Delta\bar{\sigma}^{yk}_{1} = \frac{\bar{\sigma}^{yk}_{o} - \bar{\sigma}^{y}_{*}}{\bar{\sigma}^{y}_{o} - \bar{\sigma}^{y}_{*}} \Delta\bar{\sigma}^{y}_{1} \quad ; \quad \bar{\sigma}^{y}_{o} = \sum_{k=1}^{N} \phi^{k} \bar{\sigma}^{yk}_{o} \tag{10}$$

where $\bar{\sigma}^{y}_{*}$ is a stress constant which has to be determined by a trial and error method and

$$\bar{\sigma}^{yk}_{o} = 2G\, \varepsilon^{k}_{xx} \quad \text{for} \quad k = 1,2,\ldots,N \tag{11}$$

where ε^{k}_{xx} are strains at the breakpoints of the multi-linear approximation of the stress-strain curve (Fig. 2).
The strain constants, $\bar{\varepsilon}^{k}_{1}$, (Eq. (5)) are assumed equal for all fractions:

$$\bar{\varepsilon}^{k}_{1} = \bar{\varepsilon}_{1} \tag{12}$$

and $\bar{\varepsilon}_{1}$ is taken from Fig. 9.

For $\bar{\sigma}^{y}_{*} = 0$, $\Delta\bar{\sigma}^{yk}_{1}$ is proportional with initial yield stresses $\bar{\sigma}^{yk}_{o}$. When $\bar{\sigma}^{y}_{*} = \bar{\sigma}^{y1}_{o}$, the increment of strain hardening in the first volume fraction becomes zero. In the other volume fractions $\Delta\bar{\sigma}^{yk}_{1}$ is proportional with the stress quantity $(\bar{\sigma}^{yk} - \bar{\sigma}^{y1})$.

A prediction based on this hardening distribution is given in Fig. 11. In this way we approximate that the elastic range becomes smaller when the number of cycles increases.

Volume fraction ϕ^{k} can be obtained from a multi-linear approximation of an initial stress-strain curve (Fig. 2) with the following recurrent equations:

$$\sum_{k=1}^{q} \phi^{k} (1 - h^{k}_{qm}) = 1 - \frac{s_{xx(q+1)} - s_{xx(q)}}{2G(e_{xx(q+1)} - e_{xx(q)})} \quad \text{for } q = 1,2,\ldots,N-1 \tag{13}$$

where the sum of the N volume fractions is unity, h^{k}_{qm} is the mean value of h^{k} in the strain interval of $e_{xx(q)}$ to $e_{xx(q+1)}$ and q is breakpoint number.

The necessary conversion formulae are:

$$s^{k}_{xx} = 2/3\, \sigma^{k}_{xx} \quad ; \quad e^{k}_{xx} = \varepsilon^{k}_{xx} - \frac{1 - 2\nu}{3E} \sigma^{k}_{xx} \quad \text{(tension curve)} \tag{14}$$

$$s^{k}_{xx} = 2/\sqrt{3}\, \tau^{k}_{xy} \quad ; \quad e^{k}_{xx} = 2/\sqrt{3}\, \varepsilon^{k}_{xy} \quad \text{(torsion curve)} \tag{15}$$

In the second procedure, parameters may theoretically be obtained from cyclic deformation tests as is shown in Fig. 3 [3]. The strain range of interest is subdivided into a number of straight lines (Fig. 2) such that the strains at breakpoint ε^{k} for k = 2,..,N are equal to the strain amplitudes applied in the cyclic test of Fig. 3. The experiment was done as follows. At first a cyclic deformation with strain amplitude ε^{2}_{xx} was imposed on the specimen up to the point of saturation. During this deformation only the first fraction yields. The parameters of the first fraction can be determined from this test. After this part of the

test the strain amplitude is increased till ε^{3}_{xx} and so on.
When the amount of hardening during straining with amplitude ε^{k}_{xx} is denoted by $\Delta\bar{\sigma}^{k}_{1}$ (Fig. 4) then $\Delta\bar{\sigma}^{yk}_{1}$ becomes:

$$\Delta\bar{\sigma}^{yk}_{1} = \frac{\Delta\bar{\sigma}^{k}_{1}}{\phi^{k}} \tag{16}$$

Fig. 4 also shows that $\Delta\bar{\sigma}^{k}_{1}$ obtained from separate constant strain amplitude tests are the same as those of the block-wise increasing amplitude test.

Since hardening parameter h^{k} is zero after saturation of hardening in the volume fractions $\ell < k$, the size of the volume fractions are determined by the relation:

$$\phi^{k} = 1 - \sum_{\ell=1}^{k-1} \phi^{\ell} - \frac{1}{2G} \frac{\Delta s^{k}_{xx}}{\Delta e^{k}_{xx}} \quad \text{for } k = 1,\ldots,N-1 \tag{17}$$

where $\Delta s^{k}_{xx} / \Delta e^{k}_{xx}$ is the final slope at saturation at maximum load.

If it takes n_1 cycles to reach a stress increase of $0.63\ \Delta\bar{\sigma}^{k}$, then the accumulated plastic strain is given by:

$$\bar{\varepsilon}^{pk}_{1} = n_1 \left(2\varepsilon_{k+1} - \frac{0.74\ \Delta\bar{\sigma}^{yk}}{E}\right) \tag{18}$$

Applying this procedure on the experimental data shown in Figs 3 and 4, we found that Eqs (16) and (17) are not always valid. This can be explained as follows. The assumption that stopping of the stress increase is always due to saturation of isotropic hardening is wrong, because the stress increase can also stop when the original elastic-plastic behaviour changes into pure elastic behaviour. This makes the determination of the hardening parameters much more complicated and such a procedure is not yet completed.

5. Conclusions

Constitutive equations based on the fraction model of BESSELING with an adaption for saturating isotropic strain hardening are found also suitable for the description of softening. Qualitatively speaking, several softening effects which can be observed during plastic deformation of steels (Figs 3, 6 and 8) can be described with this model.

To obtain the required hardening and softening parameters, above all, cyclic deformation tests are required, preferably for a number of different strain ranges. The determination of the parameters is difficult and for the time being, can only be found in an iterative way.

For austenitic steel WN 1.4948 (during the transition from elastic to plastic behaviour (Fig. 7)) softening seems to be a minor effect, which can be approximated by assuming no hardening in the first fraction and isotropic hardening in the rest of the volume fractions according to Eq. (10).

References

[1] BESSELING, J.F. "A theory of elastic, plastic and creep deformation of an initially isotropic material showing anisotropic strain hardening, creep, recovery and secondary creep". J. Appl. Mech., 25, 529-536, (1958).

[2] MEIJERS, P., JANSSEN, G.T.M. and BOOIJ, J. "Numerical plasticity and creep analysis based on the fraction model and experimental verification for AISI 304". SMIRT, Paper L 3/9, London (1975).

[3] HUETINK, J. "Evaluation of biaxial plasticity experiments on the ferritic steel WN 1.6770". TNO-IWECO, Report no. 5031021-79-4, (1979).

[4] JANSSEN, G.T.M. "Evaluation of biaxial plasticity experiments on the austenitic steel WN 1.4948". TNO-IWECO, Report no. 5031201-80-1, (1980).

[5] JANSSEN, G.T.M. and HUETINK, J. "Experimental verification of constitutive equations for plasticity under biaxial, cyclic and non-radial loading conditions". SMIRT, Paper L 4/2, Paris (1981).

Table 1 Modelparameters

Material	WN 1.4948			WN 1.4948		
T [°C]	20.			20.		
Hardening rule	Eq. (9)			Eq. (10); $\bar{\sigma}^{y}_{*} = \bar{\sigma}^{y1}_{o}$		
E [N/mm^2]	191000.			191000.		
ν	0.28			0.28		
		[N/mm^2]	[N/mm^2]		[N/mm^2]	[N/mm^2]
ψ^1 $\bar{\sigma}^{y1}_{o}$ $\Delta\bar{\sigma}^{y1}_{1}$	0.6208	129.9	190.5	0.6169	129.9	0.0
ψ^2 $\bar{\sigma}^{y2}_{o}$ $\Delta\bar{\sigma}^{y2}_{1}$	0.2956	206.8	190.5	0.2969	208.8	326.2
ψ^3 $\bar{\sigma}^{y3}_{o}$ $\Delta\bar{\sigma}^{y3}_{1}$	0.0726	439.4	190.5	0.0753	439.4	1313.6
ψ^4 $\bar{\sigma}^{y4}_{o}$ $\Delta\bar{\sigma}^{y4}_{1}$	0.0062	2067.6	190.5	0.0078	2067.6	8224.9
ψ^5 $\bar{\sigma}^{y5}_{o}$ $\Delta\bar{\sigma}^{y5}_{1}$	0.0048	REMAINS	ELASTIC	0.0031	REMAINS	ELASTIC
$-k$ ε [mm/mm] $k = 1,\ldots,5$	0.135			0.135		

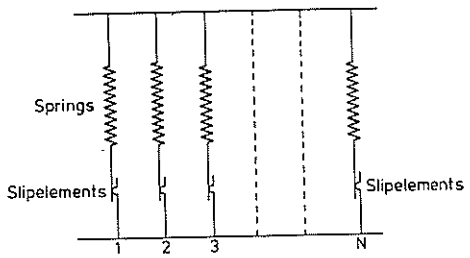

Fig. 1 Model for time-independent plastic deformation

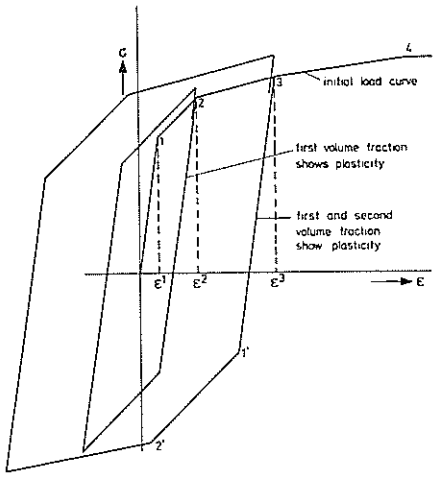

Fig. 2 Multilinear representation of a stress strain curve

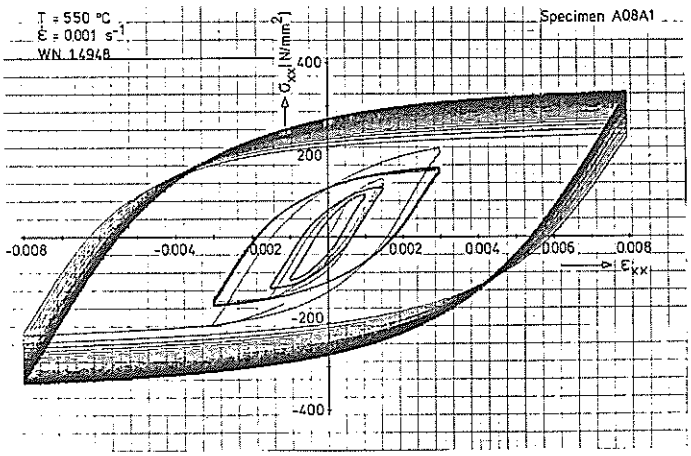

Fig. 3 Strain controlled cyclic test showing strain range depended hardening effects

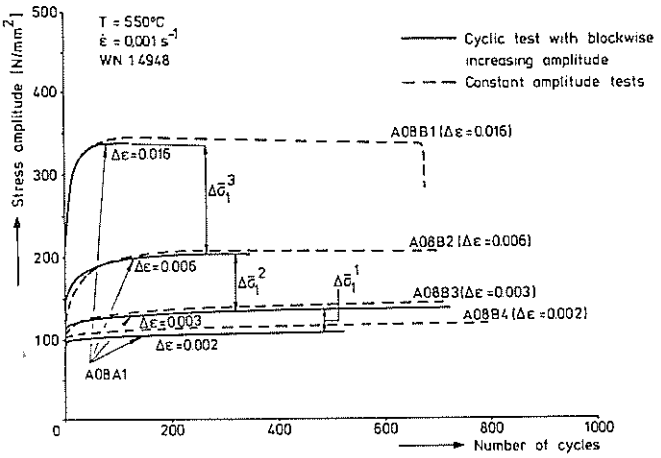

Fig. 4 Cyclic hardening curves

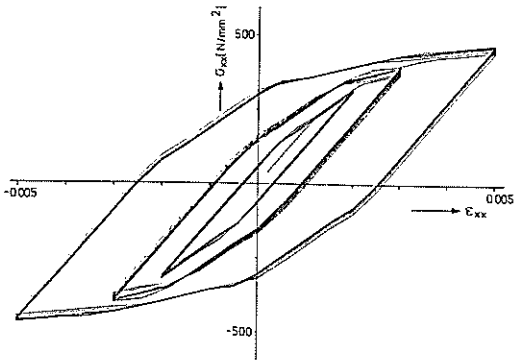

Fig. 5 Prediction of strain range depended hardening

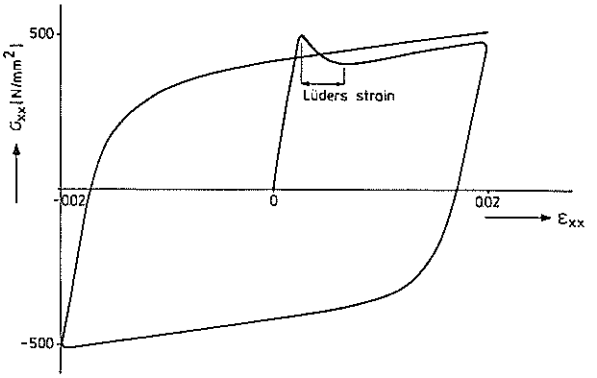

Fig. 6 Push-pull test on mild steel

$E = 196000\ N/mm^2$	$\nu = 0.28$
ψ^1	1.0
$\bar{\sigma}_0^{Y1}$	200 N/mm^2
$\Delta\bar{\sigma}_1^{Y1}$	-20 N/mm^2
$\Delta\bar{\sigma}_2^{Y1}$	40 N/mm^2
$\bar{\varepsilon}_1^1$	0.0001
$\bar{\varepsilon}_2^1$	0.01

$E = 196000\ N/mm^2$	$\nu = 0.28$	
k	1	2
ψ^k	0.9	0.1
$\bar{\sigma}_0^{Yk}$	200 N/mm^2	392 N/mm^2
$\Delta\bar{\sigma}_1^{Yk}$	-20 N/mm^2	100 N/mm^2
$\bar{\varepsilon}_1^k$	0.0001	0.01

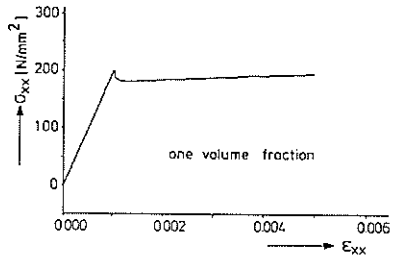

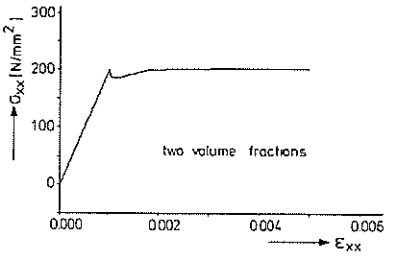

Fig. 7 Simulation of Lüder-effect by introducing negative $\Delta\bar{\sigma}^{yk}_i$-values (pseudo material)

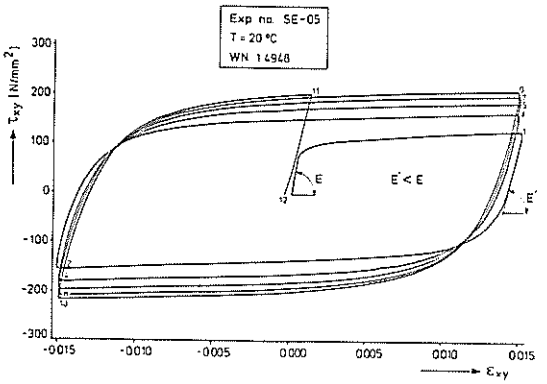

Fig. 8 Cyclic torsion test

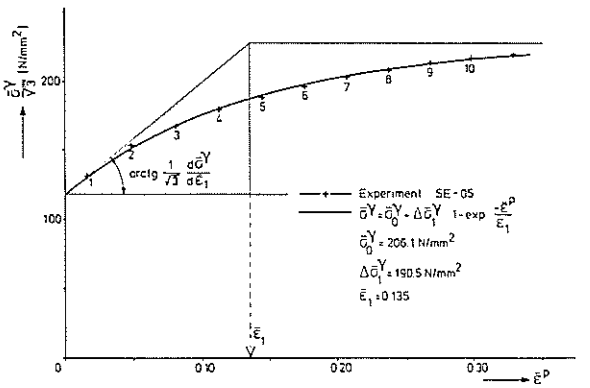

Fig. 9 Saturating isotropic strainhardening

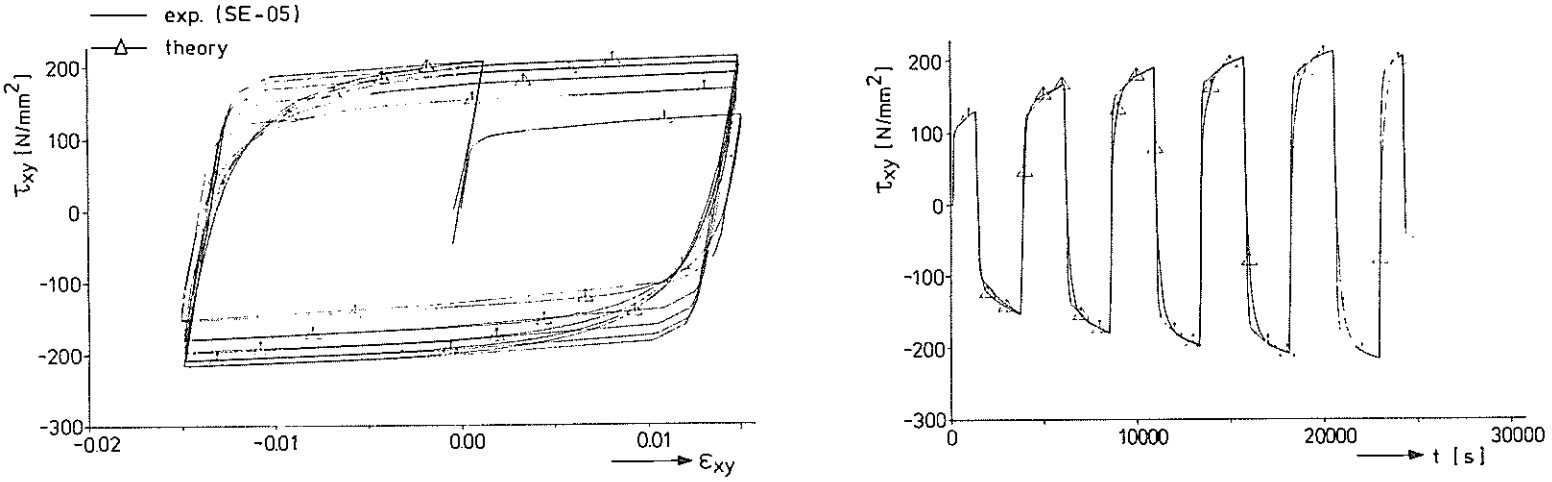

Fig.10 Cyclic torsion (strain hardening parameters are the same for all volume fractions)

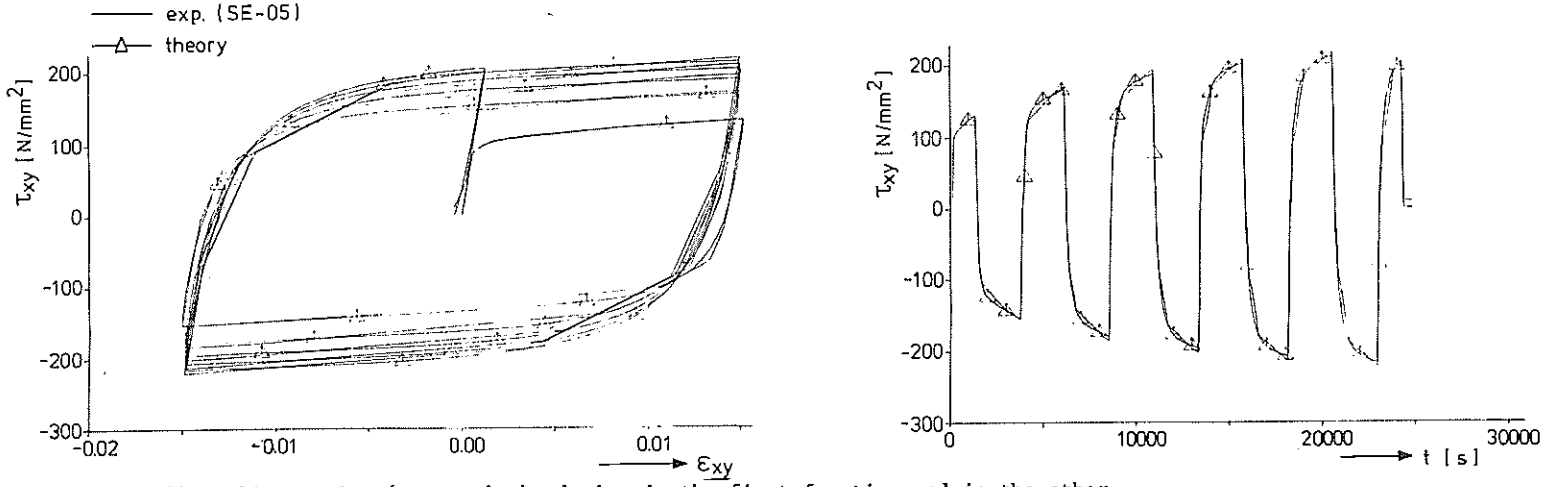

Fig. 11 Cyclic torsion (no strain hardening in the first fraction and in the other proportional with $\bar{\sigma}^{yk}_{o} - \bar{\sigma}^{yl}_{o}$)